Geophys. J. Int. (2005) **161,** 401–415 doi: 10.1111/j.1365-246X.2005.02615.x

Rigorous redatuming

W. A. Mulder

Shell International Exploration and Production, PO Box 60, 2280 AB *Rijswijk, the Netherlands*

Accepted 2005 February 9. Received 2005 February 7; in original form 2004 June 2

SUMMARY

Redatuming is an operation on seismic data that translates the positions of sources or receivers, or both. Here, redatuming is applied to shift sources and receivers to a specified depth with the aim to completely remove the effects of a complex overburden. To that end, redatuming was formulated as an inverse problem for the full acoustic wave equation, including multiples, without making simplifying assumptions such as downgoing waves or primaries only. The inverse problem is ill posed, but quite acceptable results on synthetic data were obtained with a suitable regularization.

One might expect that the redatumed result would also include waves that move up into the overburden and are reflected back to the redatuming depth. It turns out that these waves are automatically removed by the redatuming, without the need for special filters or up–down decomposition.

Key words: complex overburden, multiple elimination, redatuming, seismic processing.

1 INTRODUCTION

Redatuming is an operation on seismic data that accounts for translations of the positions of sources or receivers, or both. It can be used for various purposes, for instance, to improve the result of imaging algorithms that require regular acquisition geometry or to remove the effects of irregular topography from the seismic data. Another application is the simplification of the processing and interpretation of data recorded in areas with a complex near-surface geology. An example is sub-basalt imaging (Martini & Bean 2002).

The simplest implementation of redatuming involves static corrections on the data by applying time-shifts. More accurate redatuming algorithms are based on the wave equation, for instance Kirchhoff redatuming (Berryhill 1979, 1984; Shtivelman & Canning 1988; Bevc 1997). Many implementations are based on traveltime corrections on the data. The traveltimes can be computed by simple analytic formulae or ray tracing or finite-difference eikonal solvers. With the continuous increase in computer power, the use of phase-shift operators or one-way wave equations is feasible. Still, these approaches usually are based on simplifying assumptions such as one-way wave propagation and primaries-only data.

Here, redatuming is formulated for the two-way wave equation. This means that events such as multiples and refractions are included. To keep the exposition simple, the method is described for constant-density acoustics, the generalization to variable-density acoustics being almost trivial. Redatuming is considered to be rigorous if, when sources and receivers are moved to some depth below a potentially complex overburden, the effect of this overburden is completely removed from the data.

In Section 2, the basic equations that describe rigorous redatuming are presented. They lead to a sequence of three ill-posed inverse problems. An approximation that is valid for short time reduces that to two inverse problems. After redatuming, shot panels are obtained with sources and receivers at the redatuming level. If these panels would have been obtained directly, for instance by measurements in a horizontal well or by numerical simulation, the panels would contain waves that were reflected both from above and from below the redatuming level. One might expect that these waves would also show up in the redatumed shot panels. It turns out, however, that the solution of the two inverse problems only contains waves that have travelled below the redatuming level and that the effect of the overburden completely disappears.

The discretization and numerical solution of the two ill-posed inverse problems is presented in Section 3. This requires a special kind of regularization. The method was applied to a 1-D and three 2-D problems based on synthetic data. Results are shown in Section 4. The main conclusions and a number of open questions are listed in Section 5.

2 THEORY

2.1 Problem statement

Consider the wave equation for constant-density acoustics

$$\hat{L}\,\hat{p}(t,\mathbf{x}) = \hat{f}(t,\mathbf{x}), \quad \hat{L} = c^{-2}(\mathbf{x})\partial_{tt} - \Delta,$$

on a domain C. Here, $\hat{p}(t,\mathbf{x})$ is the pressure, $\hat{f}(t,\mathbf{x})$ is a source term and $\hat{L}$ is the wave operator with velocity $c(\mathbf{x})$. The domain C is assumed to be surrounded by absorbing boundaries, except at $z = 0$ where we will impose the free-surface boundary condition $\hat{p} = 0$. The domain can be split into two parts by cutting it along a given depth $z_0 > 0$, resulting in a shallow part A with $0 \le z \le z_0$

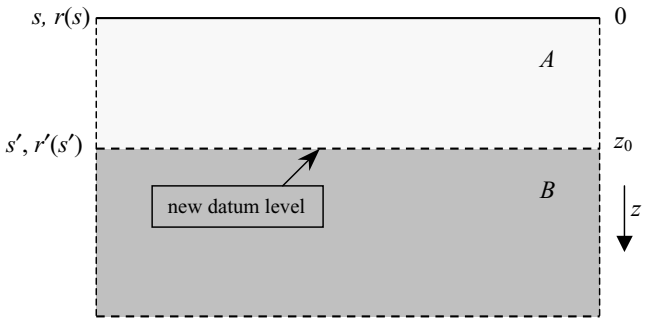

Figure 1. The domain is split into two parts, A and B. The sources s and receivers $r(s)$ are redatumed from just below the surface to a depth z_0. The dashed lines represent absorbing boundary conditions, whereas the drawn line marks a free-surface boundary condition.

and a deeper part B with $z \geq z_0$, see Fig. 1. Absorbing boundary conditions are used everywhere for these two parts, except for the free surface of domain A. Data for a shot s close to the surface can be recorded at receiver positions $r(s)$, also close to the surface. The purpose of redatuming is to find data at receiver positions $r'(s')$ for a shot s', both at a depth z_0.

We can define wave equations that have the same boundary conditions as the domain C but an absorbing condition at $z = z_0$. The wave equations and solutions inside these domains will be denoted by a superscript A, B, or C. After a Fourier transform in time, we can consider the following three wave equation problems:

$$L^V p^V = f^V = w\delta(\mathbf{x} - \mathbf{x}_V), \quad L^V = -k_V^2 - \Delta, \quad V = A, B, \text{or } C, \tag{1}$$

in the three different domains. Here, $\hat{w}(t)$ or $w(\omega)$ is the wavelet and $\mathbf{x}_V$ is the position of the source for each problem. The wave number $k = \omega/c$ and $\omega = 2\pi\nu$ for a frequency ν.

There exist numerous types of numerical absorbing boundary conditions, none of them fully satisfactory. For theoretical purposes, absorbing boundary conditions can be obtained by enlarging the domain to infinity using constant extrapolation of the model parameters in the direction perpendicular to the boundary. Note that this may be invalid for certain types of anisotropic elastic media, but these are not considered here.

2.2 Equivalent source term

In order to derive equations for redatuming, the solutions in the domains A, B and in their union C should be related to each other. This can be accomplished by means of the equivalent source term.

Consider a source fired inside domain A. For the sake of argument, this source is assumed to be located close to the surface and at a sufficiently large distance from the boundary $z = z_0$. Waves generated by this source will reach receivers located, say, near the surface (see Figs 2 and 3). The data recorded at the receivers will resemble those obtained for domain C with the same acquisition geometry. Differences arise because of waves $\hat{p}^A$ for the problem on domain A that leave through the boundary at $z = z_0$. Because this boundary is absorbing, these waves will never return to the surface in domain A. Therefore, the data difference $\hat{p}^C - \hat{p}^A$ will be related to those waves that have travelled further into the part C beyond A and were reflected back to the surface through the domain C.

Fig. 2 sketches the idea behind the equivalent source term for a 2-D problem from a different perspective. Data $\hat{p}^C$ are obtained if a shot s_C is fired in domain C and recorded at the receiver $r_C(s)$. In

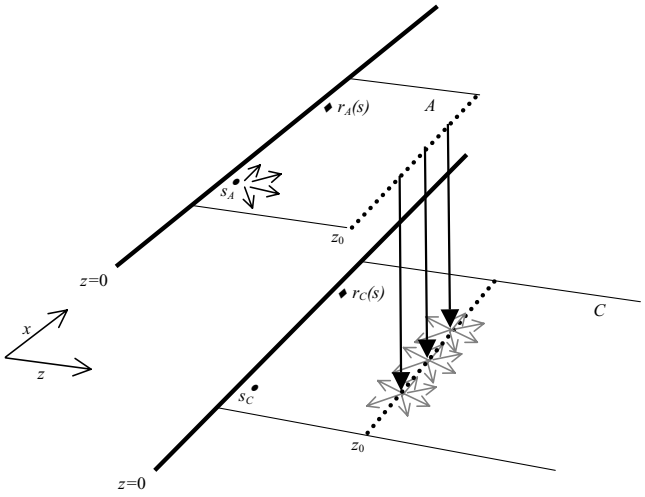

Figure 2. Data recorded at receiver r_C for a shot fired at s_C should be the same as data recorded at receiver r_A for a shot fired at s_A plus data obtained for waves that have left the domain A at the boundary $z = z_0$ and are continuing to propagate in the domain C towards the receiver r_C. The data $p^A(x', y', z_0)$ recorded in domain A on the boundary $z = z_0$ can be injected into domain C by a source term that is called the equivalent source term and will depend on the data $p^A(x', y', z_0)$.

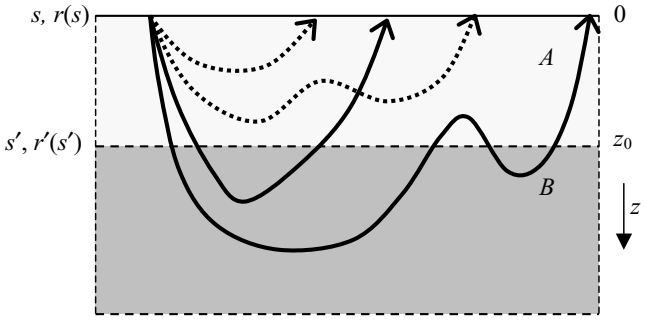

Figure 3. Waves emanating from a shot s close to the surface and recorded by receivers $r(s)$ also close to the surface, can be partitioned into waves that have travelled in the domain A only (marked by dashed arrows) and waves that have seen the domain B (marked by drawn arrows). The wave field $\hat{p}^C_{r(s)}$ recorded at the receivers can be split into $\hat{p}^A_{r(s)}$ (dashed arrows) and $\hat{p}^C_{r(s)} - \hat{p}^A_{r(s)}$ (drawn arrows).

the figure, the shot has been moved to the domain A that is a subset of C and has been relabelled s_A. The thick line is the surface. The x boundaries have been drawn as thin lines and should be thought of as being much further away from the source and receiver than suggested by the drawing. The dashed line in domain A is an absorbing boundary. The data $\hat{p}^C$ recorded at r_C for the problem in domain C with shot s_C should be the same as the sum of the data $\hat{p}^A$ recorded at r_A in domain A, and waves that have left the domain A through the boundary at $z = z_0$ and that further propagate in domain C towards $r_C(s)$, as sketched in Fig. 2. The data at $z = z_0$ from domain A can be injected into the domain C by a source term that will depend on these data. This source term is called the equivalent source term and is denoted by $f_{\text{eq}}(p^A)$ in the fourier domain. The propagation of waves from the position of the equivalent source term at $\mathbf{x}' = (x', y', z_0)$ to $\mathbf{x}_r$, the position of $r_C(s)$, is captured by the Green's function $p^{C,0}(\mathbf{x}', \mathbf{x}_r)$. The zero superscript for $p^{C,0}$ is used to stress the absence of a wavelet, or, more precisely, the use of a delta function $\delta(t)$ as wavelet. With a wavelet w, the pressure field is

$p^C = wp^{C,0}$. With these definitions, the data $p^C(\mathbf{x}_s, \mathbf{x}_r)$ recorded near the surface are given by

$$p^C(\mathbf{x}_s, \mathbf{x}_r) = p^A(\mathbf{x}_s, \mathbf{x}_r) + \int_C dx'dy'dz' f_{\text{eq}}\left(p^A(\mathbf{x}_s, \mathbf{x}')\right) p^{C,0}(\mathbf{x}', \mathbf{x}_r). \tag{2}$$

Note that reciprocity implies that arguments can be interchanged, so $p^C(\mathbf{x}_s, \mathbf{x}_r) = p^C(\mathbf{x}_r, \mathbf{x}_s)$ and so on.

A derivation of the equivalent source term $f_{\text{eq}}(p^A)$, which depends on the solution p^A for domain A, is given in Appendix A. The result is

$$f_{\text{eq}}(p^A) = -(\partial_z p^A)\delta(z - z_0) - p^A\delta'(z - z_0). \tag{3}$$

The data difference at the receiver thereby becomes

$$p^C(\mathbf{x}_s, \mathbf{x}_r) - p^A(\mathbf{x}_s, \mathbf{x}_r) = \int_{z=z_0} dx'dy' \left[p^A(\mathbf{x}_s, \mathbf{x}')\partial_z p^{C,0}(\mathbf{x}', \mathbf{x}_r) - p^{C,0}(\mathbf{x}', \mathbf{x}_r)\partial_z p^A(\mathbf{x}_s, \mathbf{x}')\right]. \tag{4}$$

If the wave fields p^A and p^C were obtained with the same wavelet $w(\omega)$, eq. (4) can be shortened to

$$w\left[p^C_{r(s)} - p^A_{r(s)}\right] = \mathcal{B}\left(p^A_{s'(s)}, p^C_{s'(r)}\right) = \int_{z=z_0} dx'dy' \left[p^A_{s'(s)}\partial_z p^C_{s'(r)} - p^C_{s'(r)}\partial_z p^A_{s'(s)}\right]. \tag{5}$$

Here, $p^V_{r(s)}$ is the pressure field for the wave propagation problem in domain V for a source s and a receiver r. Note that receiver position $\mathbf{x}_r$ has been replaced by a subscript r for a given source position s denoting $\mathbf{x}_s$, and the relation between this source and receiver has been made explicit by using $r(s)$. Likewise, s' is used to abbreviate $\mathbf{x}'$ at a depth z_0. Reciprocity implies that we can interchange $r(s)$ and $s(r)$ at will.

In the next section, eq. (5) will be used for source redatuming. The observed data are $p^C_{r(s)}$, whereas $p^A_{r(s)}$, $p^A_{s'(s)}$ and $\partial_z p^A_{s'(s)}$ can be computed if the model in domain A is known. Eq. (5) then defines an inverse problem for $p^C_{s'(r)}$ and $\partial_z p^C_{s'(r)}$. Before considering this in more detail, let us first look at some properties of the integral.

The integral in eq. (5) is denoted by $\mathcal{B}(p^A_{s'(s)}, p^C_{s'(r)})$ for brevity. Here, s' disappears after integration. From eq. (5), the following properties of $\mathcal{B}(a_{s'(s)}, b_{s'(r)})$ can be found.

(i) $\mathcal{B}(a_{s'(s)}, b_{s'(r)})$ is linear in both its arguments, so it is a bilinear map.

(ii) Reciprocity of the wave field means that we can replace $r(s)$ by $s(r)$ and vice versa on the left-hand side of eq. (5). This implies that $\mathcal{B}(a_{s'(s)}, b_{s'(r)}) = \mathcal{B}(a_{s'(r)}, b_{s'(s)})$.

(iii) Applying reciprocity inside the integral leads to $\mathcal{B}(a_{s'(s)}, b_{s'(r)}) = \mathcal{B}(a_{s(s')}, b_{s'(r)}) = \mathcal{B}(a_{s'(s)}, b_{r(s')}) = \mathcal{B}(a_{s(s')}, b_{r(s')})$.

(iv) If the superscripts are swapped in eq. (5), we obtain a minus sign, so $\mathcal{B}(a_{s'(s)}, b_{s'(r)}) = -\mathcal{B}(b_{s'(s)}, a_{s'(r)})$. Using reciprocity, this means that we also have $\mathcal{B}(a_{s'(s)}, b_{s'(r)}) = -\mathcal{B}(b_{s'(r)}, a_{s'(s)})$.

(v) If $C = A$ in eq. (5), we obtain zero on the left-hand side, so $\mathcal{B}(a_{s'(s)}, a_{s'(r)}) = 0$. Note that r and s refer to two points near the surface that are not necessarily the same.

The last property means that $p^A_{s'(r)}$ lies in the null space of the linear operator $\mathcal{B}(p^A_{s'(s)}, \cdot)$, where $p^A_{s'(s)}$ is now considered to be fixed. In Fig. 4, $p^A_{s'(r)} = p^A_{r(s')}$ is sketched as a dotted line labelled 2. Further on, we will find another wave field that belongs to its null space.

An alternative derivation of eq. (5), based on Green's second identity, is presented in Appendix B. It is shorter but provides less insight.

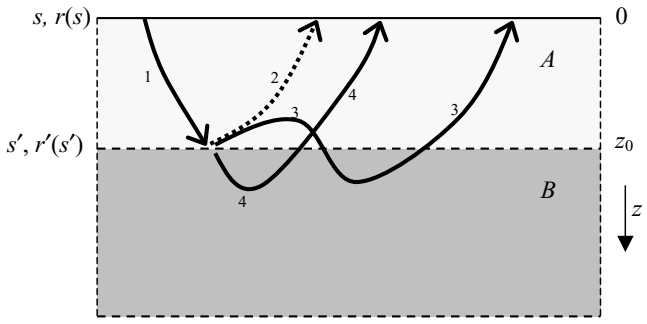

Figure 4. The equation for source redatuming (eq. 4 or eq. 5 or eq. 6) can be interpreted as follows. First, waves are created by a shot at position s close to the surface. Some of these waves, one of them marked by 1, travel through the domain A to the redatuming depth z_0. There, they control secondary sources, called the equivalent source, that radiate from positions s' into the domain C that is the union of A and B. There are waves that only pass through A to receivers $r(s')$ at the surface. One of these is marked by 2. Other waves reach the receivers passing through B, for instance those marked by 3 and 4. The dashed arrow marked by 2 represents one of the waves that disappear if the source redatuming equation is inverted.

The generalization of the above to the acoustic case is straightforward and results in an additional factor $\rho(x', y', z_0)^{-1}$ inside the integral. Here, ρ is the density.

2.3 Source redatuming

The expression derived in eq. (5) describes source redatuming. If the data for the domain C were recorded by receivers $r(s)$ near the surface and the velocity is known inside domain A, we can compute $p^A_{r(s)}$ with the same acquisition geometry as the measured $p^C_{r(s)}$. Also, $p^A_{s'(s)}$ can be computed for receivers s' at depth z_0, using the same shot positions s. Reciprocity implies that we can use $p^A_{s(s')}$ for $p^A_{s'(s)}$. Given these data, eq. (5) defines an inverse problem for $p^C_{s'(r)} = p^C_{r(s')}$ and its z derivative, $\partial_z p^C_{s'(r)}$.

In the above, it was shown that $p^A_{s'(r)}$, corresponding to the wave labelled 2 in Fig. 4, drops out of the redatuming equation. We found that $\mathcal{B}(p^A_{s'(s)}, p^A_{s'(r)}) = 0$, so eq. (5) can be rewritten as $w[p^C_{r(s)} - p^A_{r(s)}] = \mathcal{B}(p^A_{s'(s)}, p^C_{s'(r)}) - \mathcal{B}(p^A_{s'(s)}, p^A_{s'(r)}) = \mathcal{B}(p^A_{s'(s)}, p^C_{s'(r)} - p^A_{s'(r)})$, using the bilinearity of $\mathcal{B}$. This can be summarized as

$$wg_{r(s)} = \mathcal{B}\left(p^A_{s'(s)}, g_{s'(r)}\right), \quad \text{with } g = p^C - p^A. \tag{6}$$

Note that g is only defined inside the domain A.

Fig. 4 sketches the waves involved in eq. (6). On the left-hand side of this equation, we have $p^C_{r(s)} - p^A_{r(s)}$, which represents those waves for a given shot position s that have travelled through both A and B and reached the receivers $r(s)$ (see also Fig. 3). The bilinear map $\mathcal{B}$ involves the wave field $p^A_{s'(s)}$ sampled at the positions s' at a depth z_0. The arrow denoted by 1 in Fig. 4 represents $p^A_{s'(s)}$. From s', the waves continue through C, the union of A and B. Some of these waves are labelled by 2, 3 and 4. Of these, the wave 2, drawn as a dashed arrow, disappears from the redatuming equation.

In the next section, it will turn out that there are more waves that drop out of the redatuming eq. (6), meaning that $g_{s'(r)} = p^C_{s'(r)} - p^A_{s'(r)}$ cannot be recovered in full. We will postpone the discussion on the solvability of the source redatuming equation and only remark that inversion of eq. (5) or eq. (6) for $g_{s'(r)} = g_{r(s')}$ implies redatuming of the sources to a depth z_0. In Fig. 4, the arrows marked by 3 and 4 are examples of waves described by $g_{r(s')}$.

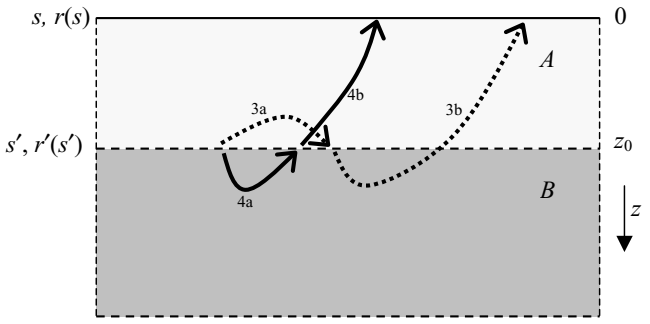

Figure 5. Eq. (8) can be interpreted as follows. Waves are created by a shot at position s' on the redatuming level. Waves can travel into A, for instance the one marked by 3a, be recorded at some receiver location $r'(s')$ and continue through domain C towards the surface, for instance as the wave marked by 3b. Alternatively, a wave can move into B, travel back to another receiver $r''(s')$, as for instance the wave marked by 4a, and continue towards the surface as 4b.

2.4 Receiver redatuming

So far, an expression (5) for source redatuming has been derived that describes the relation between data $p^C_{r(s)}$ for sources s and receivers $r(s)$ at the surface and $p^C_{r(s')}$ for sources s' at a depth z_0. Receiver redatuming requires a similar relation between data $p^C_{r(s')}$ and $p^C_{r'(s')}$ where $r'(s')$ refers to sources and receivers that are both located at a depth z_0. The derivation can be found in Appendix C. The result is

$$w\left[p^C_{r(s')} - p^A_{r(s')}\right] = \mathcal{B}\left(p^C_{r(r')}, p^B_{r'(s')} - p^A_{r'(s')}\right). \tag{7}$$

Here, r' disappears after integration. Fig. 5 may help in the interpretation of this equation. First, we rewrite eq. (7) as

$$w\left[p^C_{r(s')} - p^A_{r(s')}\right] = \mathcal{B}\left(p^A_{r'(s')}, p^C_{r(r')}\right) - \mathcal{B}\left(p^B_{r''(s')}, p^C_{r(r'')}\right). \tag{8}$$

Here, r' and r'' disappear after integration. The waves created by a source at position s' on the redatuming level move either into the domain A or the domain B. Waves travelling on the redatuming level that separates the two domains are ignored for the moment but will be considered shortly. The dotted arrow in Fig. 5 is one of the waves propagating in A. After a while, it hits a receiver $r'(s')$ and may continue to the surface where it is recorded in $r(r')$. This behaviour is described by the first term on the right-hand side of eq. (8). Here, the integration is over all r'. The second term on the right-hand side describes waves that first move into B, are recorded at $r''(s')$ and then continue to $r(s')$. One of these waves is represented by the drawn lines in Fig. 5.

Eq. (7) can be viewed as an inverse problem for $p^B_{r'(s')} - p^A_{r'(s')}$, assuming for the moment that $p^C_{r(r')}$ can be found from source redatuming. At this point, it seems that rigorous redatuming is not feasible because the presence of $p^A_{r'(s')}$ means that there are still waves that have travelled through the domain p^A.

A simplification can be made by combining eqs (6) and (7). Eq. (7) can be rewritten as

$$\begin{aligned} w\left[p^C_{r(s')} - p^A_{r(s')}\right] = {} & \mathcal{B}\left(p^C_{r(r')}, p^B_{r'(s')} - p^{B,\mathrm{dir}}_{r'(s')}\right) \\ & - \mathcal{B}\left(p^C_{r(r')}, p^A_{r'(s')} - p^{A,\mathrm{dir}}_{r'(s')}\right), \end{aligned} \tag{9}$$

where $p^{B,\mathrm{dir}} = p^{A,\mathrm{dir}}$ are the direct waves. For homogeneous models, these are clearly the direct arrivals from s' to r' at depth z_0. In the general case, these events may be defined as waves travelling on the plane of intersection of A and B, which is just the redatuming level $z = z_0$. In Appendix D, it is shown that the term $\psi_{r(s')} = \mathcal{B}(p^C_{r(r')}, p^A_{r'(s')} - p^{A,\mathrm{dir}}_{r'(s')})$ lies in the null space of $\mathcal{B}(p^A_{s'(s)}, \cdot)$, meaning that $\mathcal{B}(p^A_{s'(s)}, \psi_{r(s')}) = 0$, so it drops out when eqs (6) and (7) are combined. We therefore have to solve two inverse problems, the first one defined by eq. (6) and the second one being

$$wg_{r(s')} = \mathcal{B}\left(p^C_{r(r')}, p^B_{r'(s')} - p^{B,\mathrm{dir}}_{r'(s')}\right). \tag{10}$$

Because $p^A_{r'(s')}$ has now disappeared, rigorous redatuming is feasible! No up–down decomposition or special filter operators are needed to remove waves that have passed to the overburden above the redatuming level because they automatically drop out.

Using computed data for p^A, eq. (6) can be solved for $g_{r(s')}$. The solution of eq. (10) requires $p^C_{r(r')}$. There are a number of options.

(i) Use the solution of the first inverse problem (6) to find $p^C_{r(r')} = p^A_{r(r')} + g_{r(r')}$. Unfortunately, this is wrong as the contribution from $\mathcal{B}(p^C_{r(r')}, p^A_{r'(s')} - p^{A,\mathrm{dir}}_{r'(s')})$ is not included because it lies in the null space of $\mathcal{B}(p^A_{s'(s)}, \cdot)$ in eq. (6).

(ii) Solve eq. (6) with p^A computed by using a zero Dirichlet boundary condition [zero pressure at z_0, so $p^A_{s'(s)} = 0$], leading to a potentially less ill-posed problem in $p^C_{r(r')}$ only. Repeating the same with a Neumann boundary condition at z_0 [zero z derivative, so $\partial_z p^A_{s'(s)} = 0$] will provide $\partial_z p^C_{r(r')}$ after inversion.

(iii) Approximate $p^C_{r(r')}$ by $p^A_{r(r')}$. If z_0 lies sufficiently deep, this approximation is exact for times shorter than the traveltime from z_0 to the surface.

The last approach was used in the examples presented later on and requires the inversion of $p^B_{r'(s')} - p^{B,\mathrm{dir}}_{r'(s')}$ from

$$wg_{r(s')} \simeq \mathcal{B}\left(p^A_{r(r')}, p^B_{r'(s')} - p^{B,\mathrm{dir}}_{r'(s')}\right). \tag{11}$$

We end this section by noting that two elements of the null space of $\mathcal{B}(p^A_{s'(s)}, \cdot)$ have been found, namely $p^A_{s'(r)}$ and $\psi_{s'(r)} = \mathcal{B}(p^C_{r(r')}, p^A_{r'(s')} - p^{A,\mathrm{dir}}_{r'(s')})$. These correspond precisely to the waves that should disappear from the redatuming equations if all effects from the overburden have to be removed.

3 NUMERICAL SOLUTION

3.1 Discretization

If the velocity is known exactly inside the domain A (the shallow part of domain C), we can compute the required wave field p^A for any source–receiver pair inside A, for instance with a finite-difference scheme. Suppose the computational domain has a uniform equidistant grid with vertical spacing Δz. The redatuming level z_0 can be chosen half way between two grid points. With the discretization

$$\begin{aligned} a(x, y, z_0) \quad &= [a(x, y, z_0 - \Delta z) + a(x, y, z_0 + \Delta z)]/2, \\ \partial_z a(x, y, z_0) &= [a(x, y, z_0 + \Delta z) - a(x, y, z_0 - \Delta z)]/\Delta z \end{aligned},$$

the discrete form of eq. (5) becomes

$$w\left[p^C_{r(s)} - p^A_{r(s)}\right] = \text{Const.} \sum_{x_{s'}, y_{s'}} \left[p^A_{s'_-(s)} p^C_{r'(s'_+)} - p^A_{s'_+(s)} p^C_{r(s'_-)}\right]. \tag{12}$$

Here, $s'_\pm$ denotes a source or receiver at position $(x'_s, y'_s, z_0 \pm \frac{1}{2}\Delta z)$. The summation is carried out over a uniform grid of these sources, with a spacing that is of the order of the grid size. This spacing may be slightly larger than the grid spacing used in a finite-difference scheme, but should probably be small with respect to the typical

wavelengths to avoid spatial aliasing effects. The constant is determined by the vertical grid spacing and the horizontal spacing of the sources s'. Note that the discrete derivatives that have gone into eq. (12) are no longer evident.

The discretization in eq. (12) can also be obtained directly from a standard second-order discretization of the wave equation by deriving the equivalent source term for the discrete case, as shown in Appendix E. That approach allows for a generalization to higher-order finite-difference or finite-element discretizations.

Eq. (12) can be viewed as a linear system of equations in $p^{\mathrm{C}}_{r(s'_\pm)}$, involving a matrix $\mathbf{M}$ with coefficients

$$\mathbf{M}_{s,s'_\pm} = \pm\mathrm{Const.}\, p^A_{s'_\mp(s)}. \tag{13}$$

Using eq. (6) instead of eq. (5), we have to solve the linear system

$$w g_{r(s)} = \sum_{s'_\pm} \mathbf{M}_{s,s'_\pm} g_{r(s'_\pm)}, \tag{14}$$

for all s and $r(s)$ and for each frequency. The matrix $\mathbf{M}$ is singular with, for instance, $p^A_{r(s')}$ in its null space. If the singular problem is treated as a least-squares problem and solved by the conjugate gradient method, the first iteration produces a result that resembles classic redatuming for a zero initial guess of the solution:

$$p^C_{r(s'_\pm)} \propto \sum_s \left[p^A_{s'_\mp(s)}\right]^* g_{r(s)}. \tag{15}$$

The asterisk denotes the complex conjugate. The summation is now over s as we are using the conjugate transpose of the matrix. The resulting formula is almost the same as the one obtained in Berkhout (1997) for 'focusing in emission', without, however, making assumptions on one-way wave propagation and primaries only. Likewise, the approximation in eq. (11) leads to a formula that corresponds to 'focusing in detection'.

3.2 Inversion

First, consider the inverse problem (14) for the 1-D case. Recall that $g = p^C - p^A$. We now have a single source s and single receiver $r(s)$, but two points $s'_\pm$. Therefore, eq. (14) is singular because, for each frequency, there is one equation but two unknowns $g_{r(s'_\pm)}$. If the equation is solved iteratively by using a conjugate gradient method or directly by a truncated singular-value decomposition (TSVD), a minimum-norm solution is obtained. Unfortunately, this minimizes the size of $g_{r(s'_\pm)}$, leading to large errors in $g_{r(s')} = \frac{1}{2}[g_{r(s'_-)} + g_{r(s'_+)}]$. Better results were obtained by using another norm for the minimum-norm solution, namely $|g(z_0)|^2 + \beta^{-2}|\partial_z g(z_0)|^2$. When using the TSVD, this can be accomplished by formulating the inverse problem with g and $\gamma^{-1}\partial_z g$ as unknowns. The linear system in 1-D then has the form

$$\begin{pmatrix} m_1 & \gamma m_2 \end{pmatrix} \begin{pmatrix} g \\ \gamma^{-1}\partial_z g \end{pmatrix} = r \tag{16}$$

and the use of its TSVD results in the minimum-norm solution

$$g = m_1^* r/\left(|m_1|^2 + \gamma^2|m_2|^2\right), \quad \partial_z g = \gamma^2 m_2^* r/\left(|m_1|^2 + \gamma^2|m_2|^2\right). \tag{17}$$

Details can be found in Appendix F. Again, the asterisk denotes the complex conjugate. We can obtain $|\partial_z g|/|g| = |m_1|/|m_2| = |\partial_z p^A|/|p^A|$ by choosing $\beta = \gamma = |\partial_z p^A|/|p^A|$. For 1-D wave propagation, we hereby find that the inverse problem for rigorous redatuming does not have a unique solution. However, the regularization defined by the choice of β may still provide acceptable results.

In more than one space dimension, the linear system for shot redatuming involves a set of shots and receivers:

$$w g_{r(s)} \propto \sum_{s'} m_{1,s'(s)} g_{r(s')} + m_{2,s'(s)} \partial_z g_{r(s')}, \tag{18}$$

where

$$m_{1,s'(s)} = \left[p^A_{s'_-(s)} - p^A_{s'_+(s)}\right]/\Delta z \simeq -\partial_z p^A_{s'(s)}$$

and

$$m_{2,s'(s)} = \left[p^A_{s'_-(s)} + p^A_{s'_+(s)}\right]/2 \simeq p^A_{s'(s)}.$$

The singular behaviour of this problem is less clear. On the one hand, the fact that there are many sources s for a single source–receiver pair $r(s')$ will reduce the ill-posed character of the inverse problem. On the other hand, finite aperture effects will play a role in two ways. First, the assumption that the pressure vanishes at the sides of the domain will be violated. Secondly, illuminations effects will cause the solution for some receivers to be better defined than for others. Therefore, a suitable regularization is still required. In the examples, the same regularization is used as in the 1-D case, with a single value of γ for each frequency. Better results might be achievable with local values of γ, dependent on subsurface position and perhaps also on source and receiver positions, but this has not yet been investigated.

4 EXAMPLES

4.1 1-D example

A 1-D example is based on the marine velocity model displayed in Fig. 6. Data were computed with an 8th-order in space, 2nd-order in time-domain finite-difference code (Mulder 1997; Mulder & Plessix 2002) on a grid with 2.5 m spacing. The source and receiver were placed at 10 m depth below the free surface and 5 s of data were recorded.

For the redatuming, a depth $z_0 = 1998.75$ m was chosen and $\hat{p}^A_{r(s'_\pm)}$ was computed at depths of 1997.5 and 2000 m, respectively, using the original model down to 2 km and continuing with a constant velocity model at larger depths. The free-surface boundary condition was included. First, the source was redatumed and then the receiver. For the TSVD, values smaller than 10^{-3} times the maximum singular

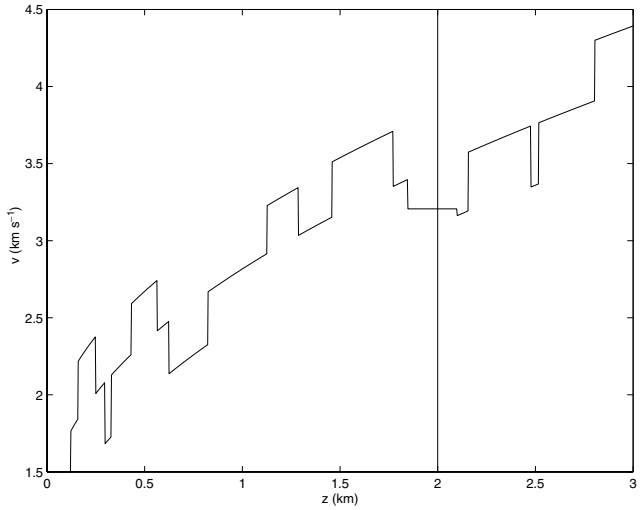

Figure 6. Velocity model for the 1-D case. The original data were obtained for a shot and receiver just below the free surface at zero depth. The redatuming level is at 2 km depth.

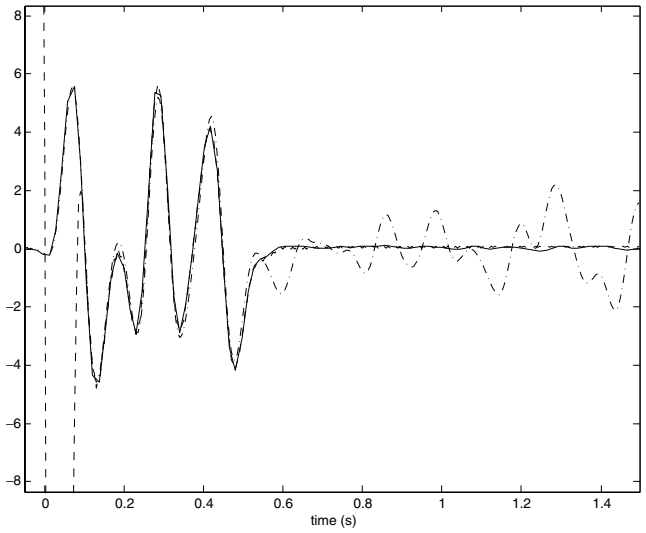

Figure 7. Result after redatuming both the source and receiver to a depth of 2 km (drawn line). The dashed line is the exact result $\hat{p}^B$, including the direct wave. The redatumed and exact result agree quite well. The fact that the direct way does not show up in the redatumed result is predicted by the theory. For comparison, the dash-dotted line represents the exact $\hat{p}^C - \hat{p}^A$, computed for a shot and receiver at the redatuming depth. This gives an indication of the waves that have travelled through the domain A above the redatuming level. These are removed by the redatuming.

value over all frequencies were set to zero. This mainly suppresses the effect of the higher frequencies that have small amplitudes and contain more numerical noise than the lower frequencies.

The resulting redatumed trace is shown in Fig. 7. For comparison, $\hat{p}^B$ is shown as well. The latter has been computed with the finite-difference code in a model that is constant for depths less than 2 km and identical to the original model at larger depths. The free-surface condition was replaced by an absorbing boundary condition. Apart from the direct wave, which was so strong that it has been clipped in the plot, the agreement between the redatumed result (drawn line) and the reference solution (dashed line) is remarkably good. For reference, $\hat{p}^C - \hat{p}^A$ has been computed with the finite-difference code and is shown as a dash-dotted line. That trace displays reflections and multiples resulting from waves that first travelled into part B of the domain, and then were reflected back and forth between the domains B and A. Note that these events have been removed by the redatuming. We conclude that the redatuming performs very well with the proposed regularization.

For comparison, we would like to include the result for classic redatuming. An obvious implementation of classic redatuming in the present context is $w(p^A)^{-1}p^C$ or $w(p^A)^{-1}(p^C - p^A)$. These operations can be regularized by replacing $(p^A)^{-1}$ with $(p^A)^*/(|p^A|^2 + \varepsilon_p^2)$, where the bias ε_p avoids division by small values. The results for both choices are displayed in Fig. 8. The second choice, $w(p^A)^{-1}(p^C - p^A)$, is markedly cleaner. Both results capture the main features of p^B in a qualitative sense.

4.2 2-D example

The method was further tested on a 2-D synthetic example. The velocity model is shown in Fig. 9. Synthetic data were created in an acoustic model with the density determined by Gardner's rule (Gardner *et al.* 1974). A free-surface boundary condition was used at the top. We chose $z_0 = 598.75$ m, which is marked by the horizontal line in the figure. Near the surface, receivers were placed at a depth of 5 m between $x = 100$ and 900 m with 10 m spacing. The sources were placed between 105 and 895 m with the same spacing and depth. Near z_0, we put receivers (or sources) between $x = 100$ and 900 m with 10 m spacing and at 597.5 and 600.0 m depth. A 2.5 m grid spacing was used and 1.5 s of data were recorded.

The result after redatuming is displayed in Fig. 10(a), for a shot at $x = 490$ and $z = 598.75$ m. Fig. 10(b) shows the exact $\hat{p}^B$, after subtraction of the direct wave, which was computed with the finite-difference code in a constant-velocity model. Fig. 10(c) represents $\hat{p}^C - \hat{p}^A$ and still includes waves that have travelled downwards from the redatuming level and were subsequently reflected back and forth between domains B and A. The redatuming operation removes these waves.

The result is less accurate than in the 1-D case. The threshold value in the TSVD had to be chosen fairly large, at 0.05 times the largest singular value over all frequencies, to obtain acceptable results. This suggests that the 2-D problem is rather ill posed. Still, the redatuming result is quite acceptable. For comparison, the results of our implementation of classic redatuming are shown in

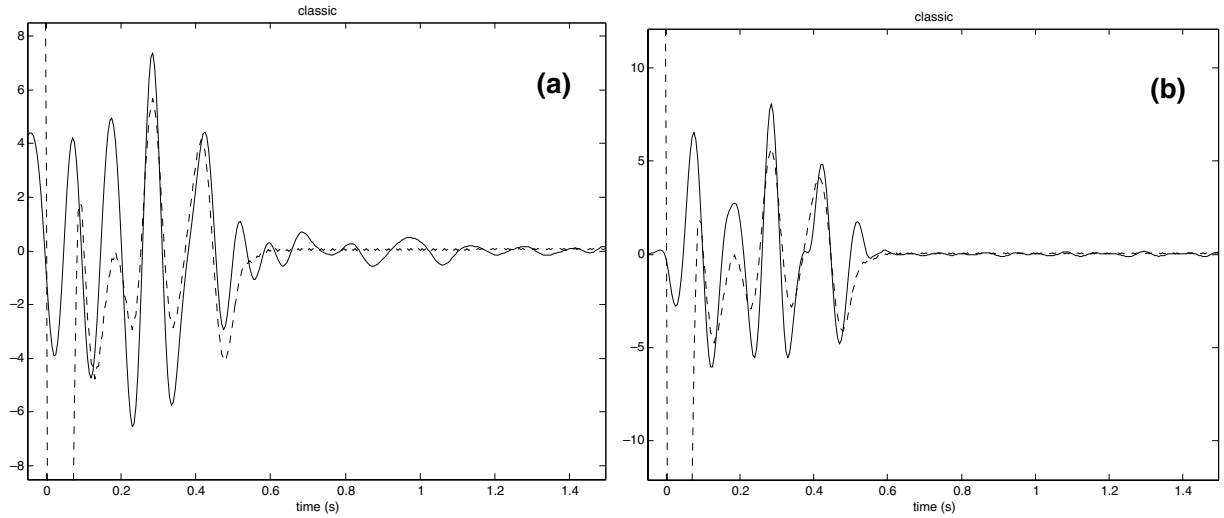

Figure 8. Result for classic redatuming based on $w(p^A)^{-1}p^C$ (a) and $w(p^A)^{-1}(p^C - p^A)$ (b) after redatuming both the source and receiver to a depth of 2 km (drawn line). The dashed line is the exact result $\hat{p}^B$, including the direct wave.

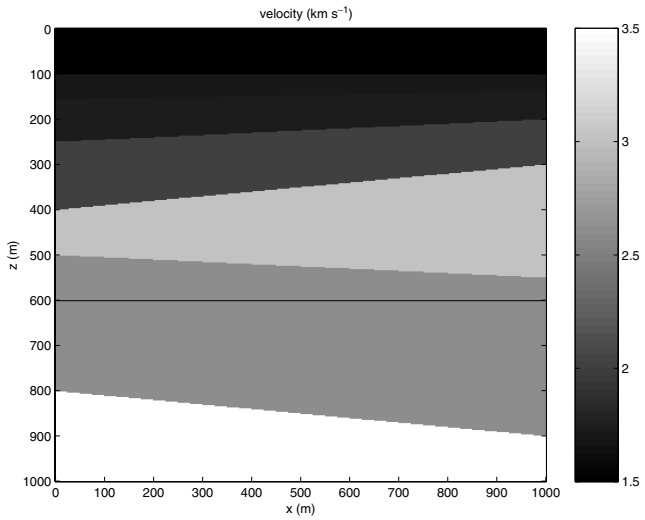

Figure 9. Velocity model for the first 2-D example. The drawn line corresponds to the redatuming level.

Fig. 11. Again, the result for $w(p^A)^{-1}(p^C - p^A)$ is cleaner than the one for $w(p^A)^{-1}p^C$. Both provide qualitatively correct results for the shorter offsets.

4.3 Sparse data

Redatuming for the last example was repeated with sparse data. A subset consisting of approximately 30 per cent of the sources and 30 per cent of the receivers near the surface was randomly selected. The redatumed result is shown in Fig. 12. The artefacts are stronger when compared with Fig. 10(a), but the main features of the single reflection event are still preserved.

4.4 Redatuming level crossing a reflector

What happens if the redatuming level crosses a reflector? Fig. 13 shows a velocity model that is a slight modification of the one used earlier. The redatuming result is displayed in Fig. 14. In the exact result $p^B - p^{B,\mathrm{dir}}$ on the right (Fig. 14b), two events are visible to the left of the source position ($x_s = 490$ m, $z_s = 598.75$ m) at trace no. 40, corresponding to the two reflectors that are present below the redatuming level. The source selected for this figure is positioned

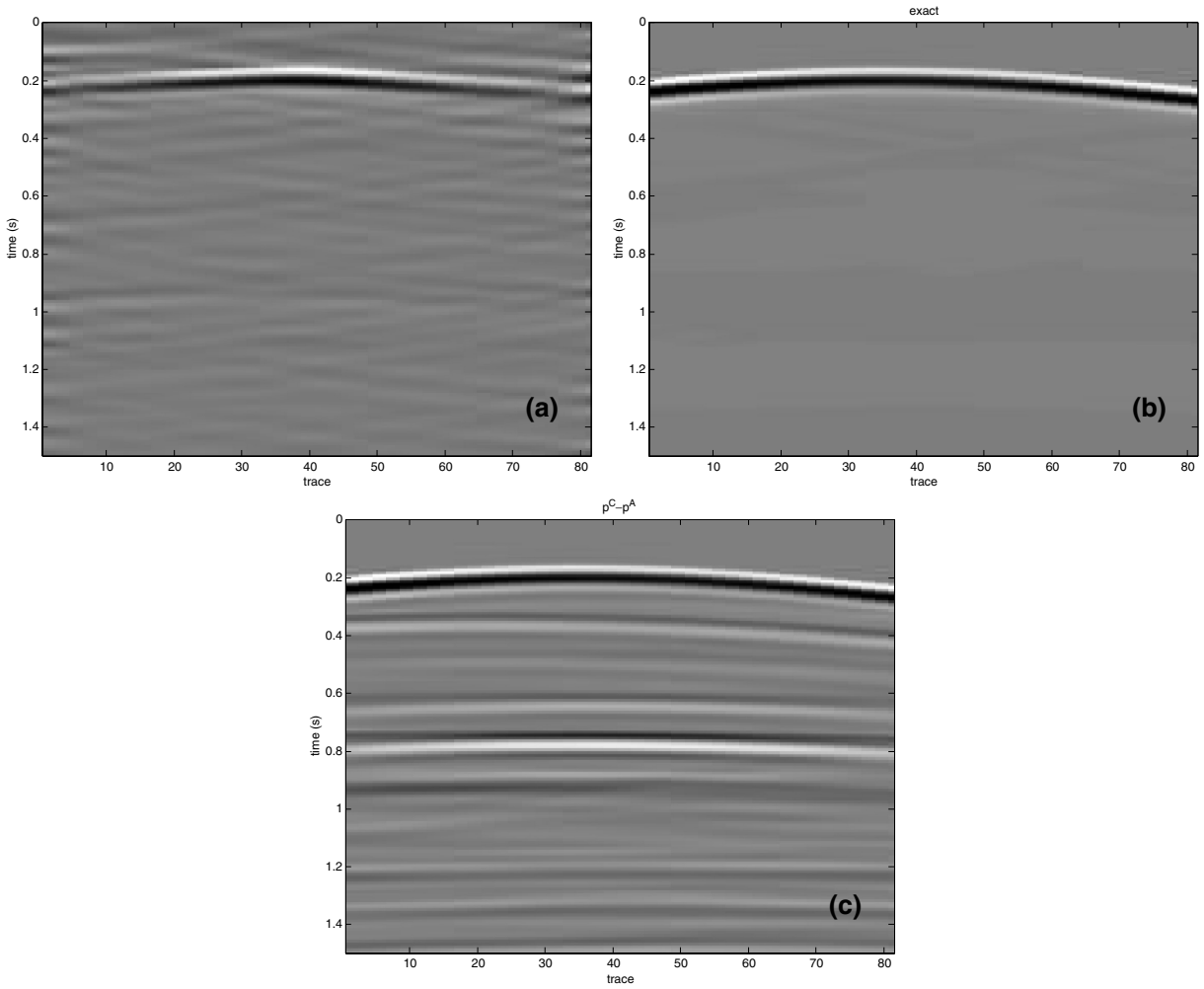

Figure 10. Redatumed shot panel (a) and exact solution with the direct wave subtracted (b). For comparison, $\hat{p}^C - \hat{p}^A$ for a shot and receivers at the redatuming depth is shown (c). The last picture contains waves that have travelled into the domain A above the redatuming level.

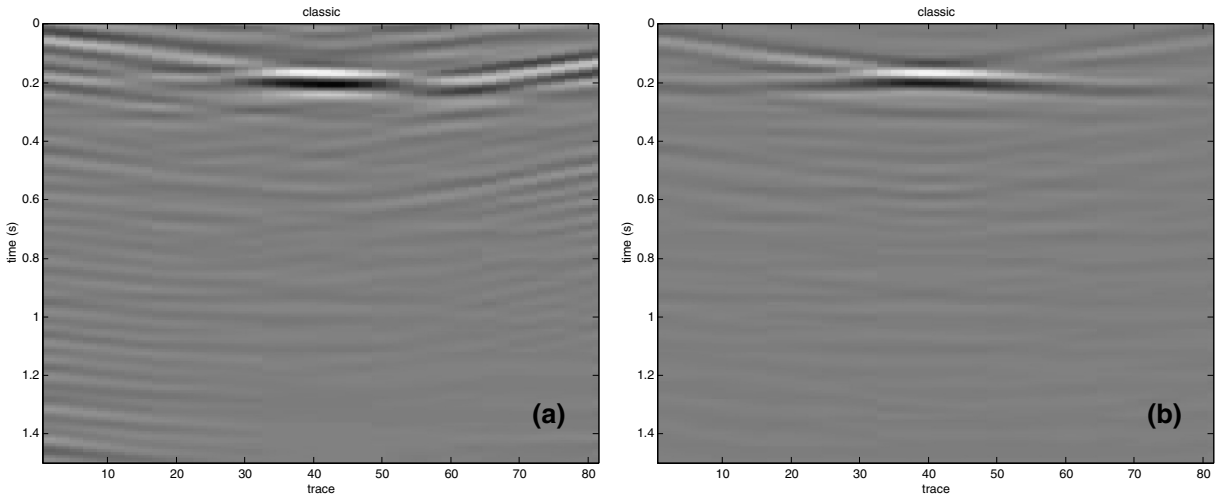

Figure 11. Result for classic redatuming based on $w(p^A)^{-1}p^C$ (a) and $w(p^A)^{-1}(p^C - p^A)$ (b).

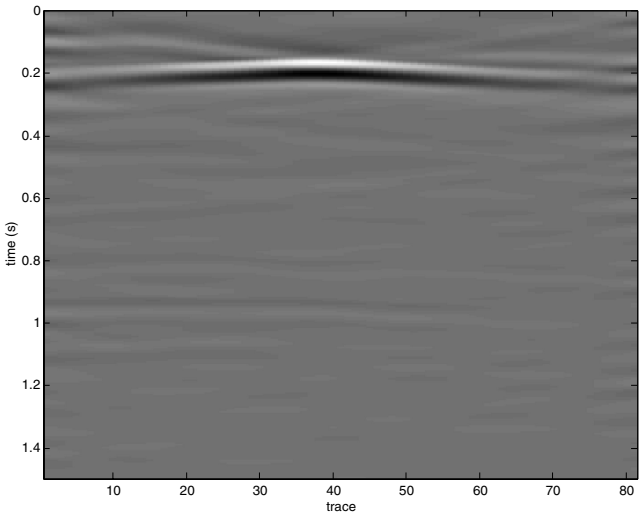

Figure 12. Redatuming result similar to Fig. 10(a), but now based on a subset of the data, using a random subset of 30 per cent of the number of shots and 30 per cent of the number of receivers near the surface.

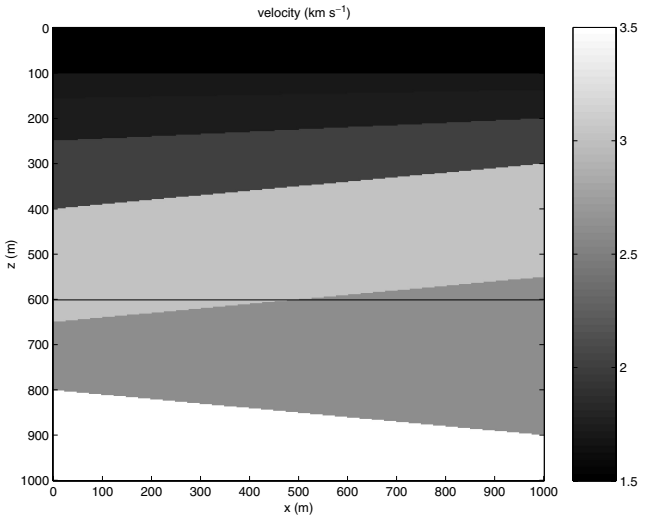

Figure 13. Model where the redatuming level, marked by the drawn line, crosses a reflector.

just above the reflector that crosses the redatuming level. A little to the right of the source, we should only see one reflector if the absorbing boundary conditions would perform perfectly well and the direct wave would have been subtracted correctly. As mentioned at the end of Section 2.1, absorbing boundaries are simulated by enlarging the domain so that artificial reflections from the domain boundaries cannot reach the receivers. The material properties, in this case the velocity, are extended into the enlarged domain by constant interpolation in the direction perpendicular to the boundary. In other words, the values at the original absorbing boundary are copied in the perpendicular direction. In the current example, this means that at the point where the reflector crosses the redatuming level, a diffractor is created when we are computing solutions for p^B. Above the redatuming level, the reflector continues as a single vertical interface. For the computation of the direct wave $p^{B,\mathrm{dir}}$, the model parameters at the redatuming depth are copied to all depths leaving just a vertical reflector on the entire domain. Fig. 14(b) shows that this approach only provides results that are approximately correct. Although most of the energy of the direct wave has been subtracted, some is still left.

The result of the redatuming is shown in Fig. 14(a). The reflection event that corresponds to the reflector crossing the redatuming level is visible close to the source, but not at larger offsets to the left. It would seem that the algorithm cannot deal very well with this situation. If, however, one would follow a ray from the redatumed source to a point of specular reflection on the nearby reflector on the left and then back to the surface, very long offsets in the surface data would be required to capture that energy. As these long offsets were not present in the surface data, one cannot expect any significant illumination of the reflector except close to the source.

4.5 A more complex 2-D example

A more challenging 2-D example is based on the velocity model shown in Fig. 15. Again, synthetic data were created in an acoustic model with the density determined by Gardner's rule (Gardner *et al.* 1974). A land-type acquisition geometry was chosen, with shots between $x = 110$ and 1890 m at a 20 m interval and at 5 m depth,

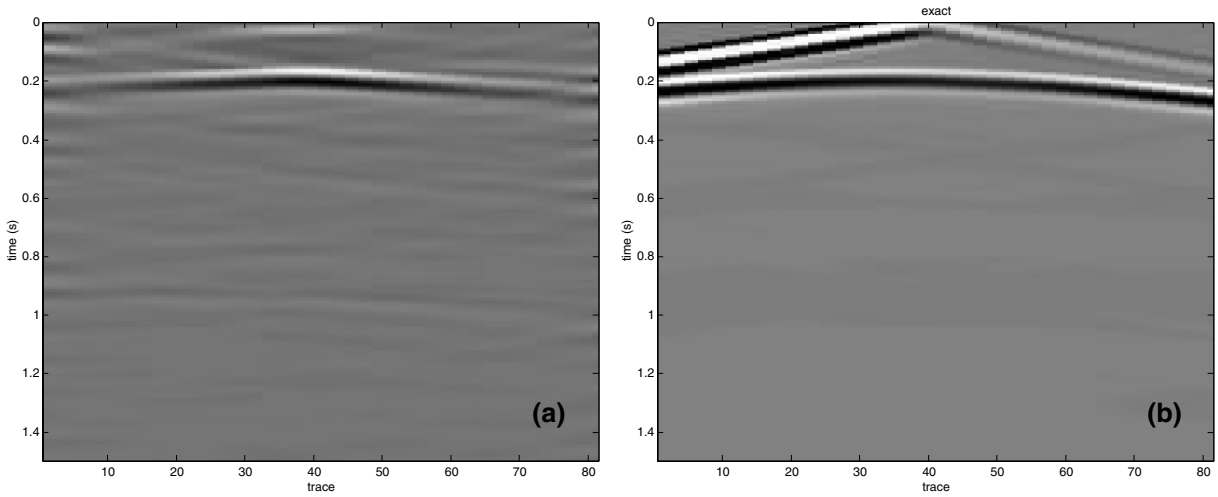

Figure 14. Redatumed shot panel (a) for a source at a position corresponding to trace no. 40, located just above the reflector that crosses the redatuming level. The exact $p^B - p^{B,\mathrm{dir}}$ is shown on the right in (b). Some of the direct-wave energy has not been properly removed on the right. The redatuming algorithm seems to have problems recovering the nearby reflector, but this is probably a result of the finite aperture.

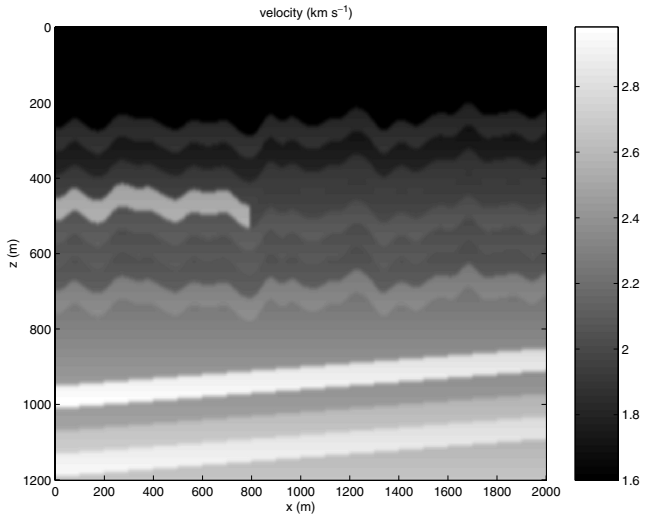

Figure 15. Velocity model for the more complex 2-D example.

and receivers between $x = 100$ and 1900 m at the same interval and depth. The computational grid had a 2.5 m spacing. The redatuming depth was chosen to be 798.75 m. The shots and receivers at the redatuming level were positioned between 100 and 1900 m with a 20 m interval.

The top panel of Fig. 16 shows the result after redatuming, for a shot at $x = 980$ m and $z = 798.75$ m. The middle panel is the exact result with the direct arrival removed, whereas the bottom panel displays $\hat{p}^C - \hat{p}^A$. The threshold value for the TSVD was 0.05 times the maximum singular value over all frequencies. The redatumed result has artefacts, in particular at larger offsets. These must be caused by finite-aperture effects. In deriving the redatuming formulae (5) and (10) or (11), the contributions to the integral from the vertical sides of the domain were assumed to vanish. This assumption is clearly violated in the current example and apparently gives rise to the observed artefacts at larger offsets. These artefacts resemble those found in migration and can be removed by similar techniques as used in migration, such as windowing, tapering and anti-alias filtering.

For comparison, the results of our implementation of classic redatuming are shown in Fig. 17. They strongly suffer from amplitude distortions. Larger values have been clipped to bring out the weaker events.

4.6 Effect of noise and model errors

To study the robustness of the redatuming algorithm, the last example was repeated with noise in two ways. First, white noise was added to the data. Secondly, the velocity model was perturbed.

The result with white noise is shown in Fig. 19(a). The amplitude of the noise was 10 per cent of the maximum amplitude of the time-domain data, which is rather large as the direct wave was included when computing the maximum. Compared to Fig. 16(a), the result is quite similar. Apparently, the redatuming method is not too sensitive to white noise.

For the model perturbation, an approach was taken that resembles the handling of real data. An initial, smooth velocity model was determined from the data by differential semblance optimization (Mulder & ten Kroode 2002). This model was used as a starting guess for an acoustic full-waveform inversion. Details for latter can be found in Mulder & Plessix (2004). The inversion was performed with a frequency-domain code, using only the lower frequencies between 10 and 20 Hz at a 0.5 Hz interval. The inversion was stopped after 30 iterations. The resulting velocity and density models are displayed in Fig. 18. The ratio between the least-squares data error (half the sum of the squared differences between synthetic and observed data) divided by the data energy was 0.14. The redatuming result is shown in Fig. 19(b). The main features are still there, but comparison with Fig. 19(a) shows timing errors. These are an indication of velocity errors in the model inversion result. Still, the main reflection events can be seen for the shorter offsets, albeit with some effort.

5 CONCLUSIONS

Formulae for rigorous redatuming have been derived for the acoustic wave equation. To accomplish the redatuming, three inversion steps need to be carried out. In the examples, an approximation that is

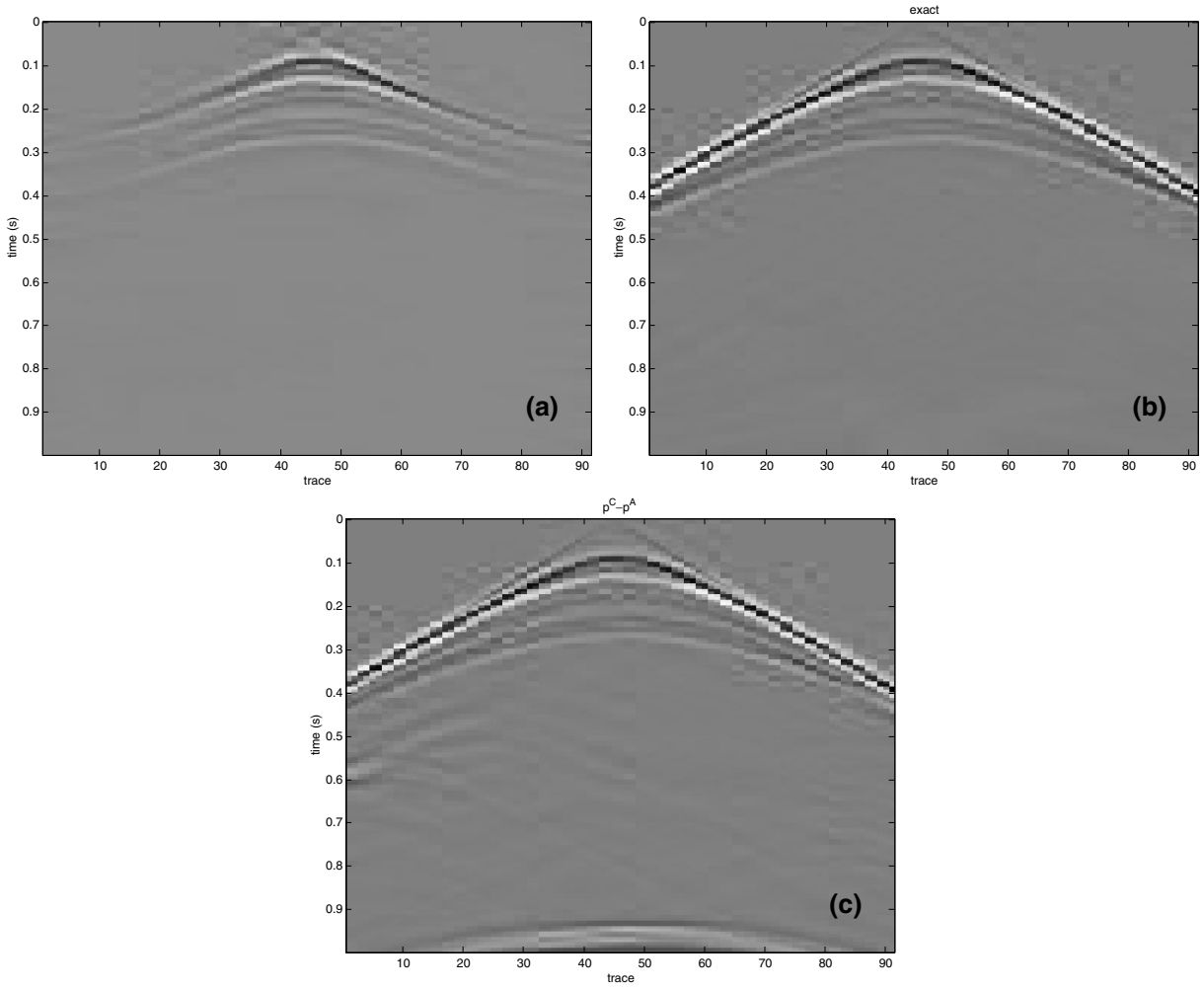

Figure 16. Redatumed shot panel (a), exact solution (b) and exact $\hat{p}^C - \hat{p}^A$ (c) for a shot and receivers at the redatuming depth for the second 2-D example.

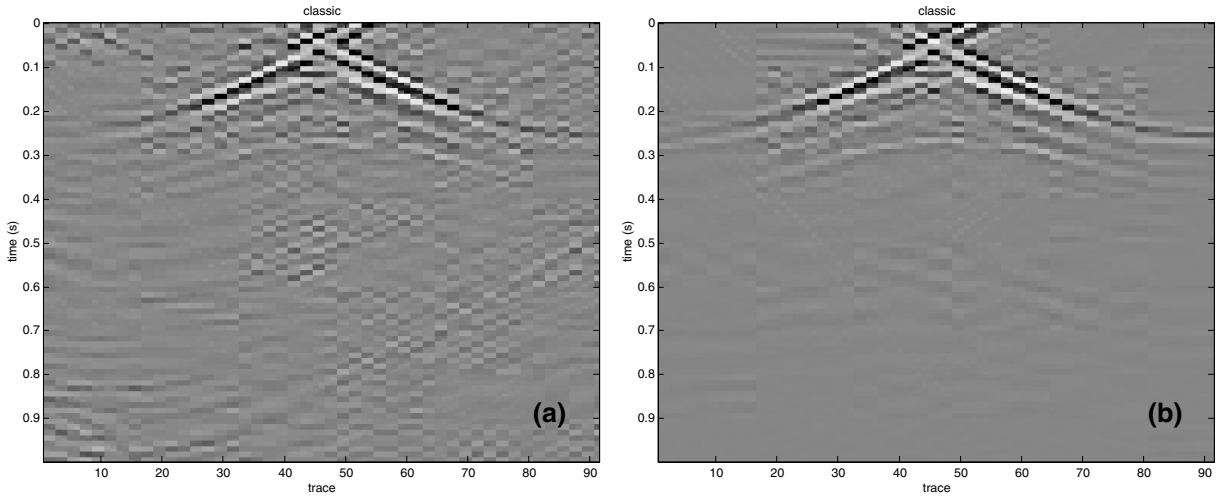

Figure 17. Result for classic redatuming based on $w(p^A)^{-1}p^C$ (a) and $w(p^A)^{-1}(p^C - p^A)$ (b).

valid for short time was used to reduce the number of inversion steps to two. The ill-posed character of the inverse problem requires a suitable regularization. Here, a regularization was proposed that leads to reasonable results, although there is room for improvement.

Potential applications of the present redatuming method are as follows.

(i) Removal of a complex overburden.
(ii) Data interpolation.

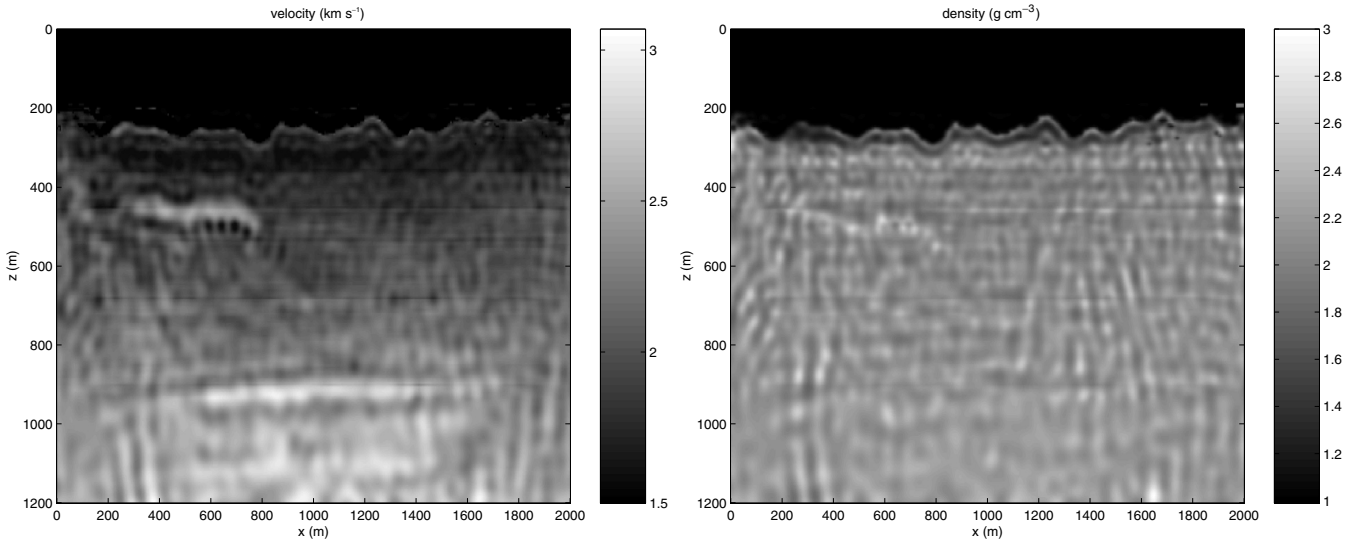

Figure 18. Velocity (left) and density (right) model for the second 2-D example, obtained after acoustic inversion.

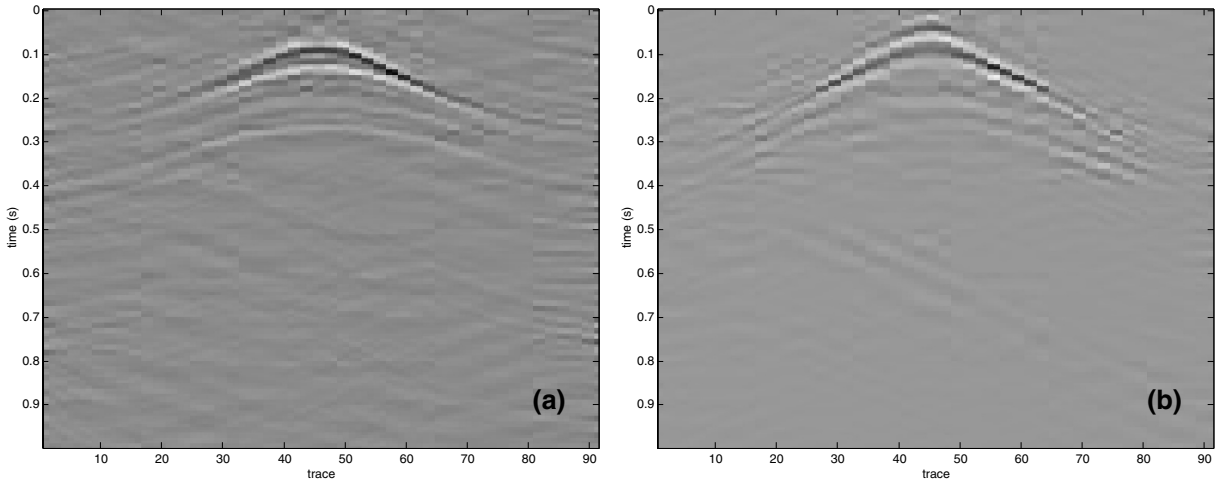

Figure 19. Results in the presence of white noise (a) and model noise (b).

(iii) Multiple removal. In a marine setting, the overburden can be taken as the sea and sea floor and some shallow structure just below the sea bottom.

(iv) Survey sinking migration and model building with layer stripping. In this case, the short-time approximation (11) should not be used.

The generalization of the redatuming equations to variable-density acoustics is straightforward and has been used in some of the examples. Solving the inverse problem for the former is similar to the constant-density case considered here. For the elastic case, the solution of the inverse problem is expected to be more difficult. Finally, it remains to be seen if the current method can be used on real data. This requires a very accurate model between the surface and the redatuming level, which may be impossible to determine in practice.

REFERENCES

Berkhout, A.J., 1997. Pushing the limits of seismic imaging, Part I: Prestack migration in terms of double dynamic focusing, *Geophysics,* **62**, 937–954.

Berryhill, J.R., 1979. Wave-equation datuming, *Geophysics,* **44**, 1329–1344.

Berryhill, J.R., 1984. Wave equation datuming before stack, *Geophysics,* **49**, 2064–2067.

Bevc, D., 1997. Imaging complex structures with semirecursive Kirchhoff migration, *Geophysics,* **62**, 577–588.

Gardner, G.H.F., Gardner, L.W. & Gregory, A.R., 1974. Formation velocity and density: The diagnostic basis for stratigraphic traps, *Geophysics,* **39**, 770–780.

Martini, F. & Bean, C.J., 2002. Interface scattering versus body scattering in subbasalt imaging and application of prestack wave equation datuming, *Geophysics,* **67**, 1593–1601.

Mulder, W.A., 1997. Experiments with Higdon's absorbing boundary conditions for a number of wave equations, *Computat. Geosci.,* **1**, 85–108.

Mulder, W.A. & ten Kroode, A.P.E., 2002. Automatic Velocity Analysis by Differential Semblance Optimization, *Geophysics,* **67**, 1184–1191.

Mulder, W.A. & Plessix, R.-E., 2002. Time- versus frequency-domain modelling of seismic wave propagation. In: *64th Mtg. Eur. Assoc. Explor. Geophys., Extended Abstracts,* Abstract No. E015. Eur. Assoc. Explor. Geophys., Houten, the Netherlands.

Mulder, W.A. & Plessix, R.-E., 2004. A comparison between one-way and two-way wave-equation migration, *Geophysics,* **69**, 1491–1504.

Shtivelman, V. & Canning, A., 1988. Datum correction by wave equation extrapolation, *Geophysics,* **53**, 1311–1322.

APPENDIX A: DERIVATION OF THE EQUIVALENT SOURCE TERM

An expression for the equivalent source term is derived. To simplify the exposition, the dependence of the solution on x and y is ignored and only 1-D wave propagation is considered. The extension to two and three dimensions is trivial. We start with a solution defined on the domain A (see Figs 2 and 3). The domain is extended beyond $z = z_0$ to infinity in such a way that no reflections occur for $z > z_0$. The wave field on this domain for a source close to the surface is denoted by p and obeys $-k^2 p - \partial_{zz} p = f(z - z_s)$, with $z_s \ll z_0$. Near $z = z_0$, $-k^2 p - \partial_{zz} p = 0$ because the source term typically resembles a delta function, so $f(z - z_s) = 0$ near z_0. At $z = z_0$, we want to construct a source $f_{\rm eq}$ that, when placed in the extension of domain A, will generate waves that are identical to those that leave the original domain A through $z = z_0$. If this wave field is denoted by q, then $q = p$ on the extension $z > z_0$ of the domain A, whereas q should be zero for $z < z_0$. Once the source that generates q has been determined, we can place it into the domain C to continue the propagation of waves that have left domain A through the boundary at $z = z_0$ (see Fig. 2). Direct application of the wave equation would lead to $f_{\rm eq} = -k^2\, q - \partial_{zz} q$. This is not correct because q is discontinuous, so we have to reformulate this problem in the weak or distributional form of the wave equation.

We start by deriving the weak form of the wave equation. If p is a solution of the wave equation with a zero Dirichlet boundary condition at the surface $z = 0$, so $p(0) = 0$, we have

$$\int_0^\infty dz\big(f + k^2 p + \partial_{zz} p\big)\phi = \int_0^\infty dz\big[(f + k^2 p)\phi + p\partial_{zz}\phi\big] = 0, \quad \text{for all } \phi \in \mathcal{D}([0,\infty)). \tag{A1}$$

Here, $\mathcal{D}([0, \infty))$ is the space of complex-valued, infinitely many times differentiable functions that are non-zero on a finite interval inside $[0, \infty)$ and are equal to zero at $z = 0$. The second integral in eq. (A1) represents the weak or distributional form of the wave equation.

To find the equivalent source term, we define a discontinuous solution q with $q = p$ for $z \geq z_0$ and $q = 0$ for $z < z_0$ and determine $f_{\rm eq}$ from

$$\int_0^\infty dz\big[\big(f_{\rm eq} + k^2 q\big)\phi + (\partial_{zz}\phi)q\big] = 0, \text{ for all } \phi \in \mathcal{D}([0,\infty)). \tag{A2}$$

Now

$$\begin{aligned} 0 = \int_0^\infty dz\,\big[\big(f_{\rm eq} + k^2 q\big)\phi + (\partial_{zz}\phi)q\big] &= \int_0^\infty dz\; f_{\rm eq}\phi + \int_{z_0}^\infty dz\,\big[k^2 q\phi + (\partial_{zz}\phi)q\big] \\ &= \int_0^\infty dz\; f_{\rm eq}\phi - [\phi(\partial_z p) - p(\partial_z\phi)]_{z_0}^\infty + \int_{z_0}^\infty dz\big(k^2 p + \partial_{zz} p\big)\phi. \end{aligned}$$

The last integral on the right-hand side vanishes if the original source term f was a delta function positioned at $z < z_0$. Recall that $\int_a^b dz\; \phi(z)\delta'(z - z_0) = -\partial_z\phi(z_0)$ if $a < z_0 < b$. Therefore,

$$f_{\rm eq}(p) = -(\partial_z p)\delta(z - z_0) - p\delta'(z - z_0). \tag{A3}$$

APPENDIX B: ALTERNATIVE DERIVATION OF THE EQUIVALENT SOURCE TERM

Given the two wave propagation problems (eq. 1) for domains $V = A$ and $V = C$, we have a wave field $p^A(\mathbf{x}_A, \mathbf{x})$ at positions $\mathbf{x}$ in domain A for a source at position $\mathbf{x}_A$ and a wave field $p^A(\mathbf{x}_C, \mathbf{x})$ with $\mathbf{x}$ in domain C for a source at position $\mathbf{x}_C$. Note that $\mathbf{x}_C$ and $\mathbf{x}_A$ do not have to coincide. By using the wave equations, it is easy to show that

$$\int_V d\mathbf{x}\,\big[p^A(\mathbf{x}_A, \mathbf{x})\Delta p^C(\mathbf{x}_C, \mathbf{x}) - p^C(\mathbf{x}_C, \mathbf{x})\Delta p^A(\mathbf{x}_A, \mathbf{x})\big] = w\,\big[p^C(\mathbf{x}_C, \mathbf{x}_A) - p^A(\mathbf{x}_A, \mathbf{x}_C)\big] + \int_V d\mathbf{x}\,\big(k_A^2 - k_C^2\big)p^A(\mathbf{x}_A, \mathbf{x})p^C(\mathbf{x}_C, \mathbf{x}). \tag{B1}$$

Here, $p^C\,(\mathbf{x}_C, \mathbf{x}_A)$ denotes the wave field p^C sampled at a receiver position $\mathbf{x}_A$, for a source at $\mathbf{x}_C$. Likewise, $p^A(\mathbf{x}_A, \mathbf{x}_C)$ denotes the wave field p^A sampled at $\mathbf{x}_C$ for a source at $\mathbf{x}_A$. Reciprocity implies that $\mathbf{x}_A$ and $\mathbf{x}_C$ can be interchanged. If $V = A$, the integral on the right-hand side vanishes. The left-hand side contains a term $p^A\partial_x^2 p^C - p^C\partial_x^2 p^A$. If we first integrate over x, we obtain

$$\int_{-\infty}^\infty dx\,\big(p^A\partial_x^2 p^C - p^C\partial_x^2 p^A\big) = \big[p^A\partial_x p^C - p^C\partial_x p^A\big]_{-\infty}^\infty.$$

If the vertical boundaries are sufficiently far away so that we can neglect the pressure there, this term vanishes. The same can be done for the y direction. For the z direction, the pressure vanishes at the surface $z = 0$, so we obtain

$$w\,\big[p^C(\mathbf{x}_C, \mathbf{x}_A) - p^A(\mathbf{x}_A, \mathbf{x}_C)\big] = \int_{z=z_0} dx dy\,\big[p^A(\mathbf{x}_A, \mathbf{x})\partial_z p^C(\mathbf{x}_C, \mathbf{x}) - p^C(\mathbf{x}_C, \mathbf{x})\partial_z p^A(\mathbf{x}_A, \mathbf{x})\big], \tag{B2}$$

or, by denoting $\mathbf{x}_C$ with s and $\mathbf{x}_A$ with r and by using reciprocity,

$$w\,\big[p^C_{r(s)} - p^A_{r(s)}\big] = \int_{z=z_0} dx' dy'\,\big[p^A_{s'(s)}\partial_z p^C_{s'(r)} - p^C_{s'(r)}\partial_z p^A_{s'(s)}\big]. \tag{B3}$$

Here, the subscript $r(s)$ indicates data recorded at a receiver r for a shot s. The points s' are located at (x', y', z_0).

B1 Remark

This application of Green's second identity differs from the more common one with the complex conjugate, using $\int_V d\mathbf{x}[(p^A)^*\Delta p^C - (\Delta p^A)^* p^C]$.

APPENDIX C: RECEIVER REDATUMING

A derivation for the formula describing receiver redatuming can be given along the lines of Appendix B. The source s' is located at a depth z_0, the receivers $r(s')$ are positioned near the surface (or anywhere inside domain A) and the redatumed receivers $r'(s')$ are placed at a depth z_0. Instead of eq. (B1) with $V = A$, we find

$$\int_A d\mathbf{x}\left[p^A(\mathbf{x}_A, \mathbf{x})\Delta p^C(\mathbf{x}_C, \mathbf{x}) - p^C(\mathbf{x}_C, \mathbf{x})\Delta p^A(\mathbf{x}_A, \mathbf{x})\right] = w\left[\tfrac{1}{2}p^C(\mathbf{x}_C, \mathbf{x}_A) - p^A(\mathbf{x}_A, \mathbf{x}_C)\right]. \tag{C1}$$

Again, $p^C(\mathbf{x}_A)$ denotes the wave field p^C sampled at a receiver position $\mathbf{x}_A$, for a source at $\mathbf{x}_C$, but now $\mathbf{x}_A$ represents s' and has $z_A = z_0$. Because the associated delta function sits on the boundary of the domain, a factor $\frac{1}{2}$ is obtained after integration over the domain A. The position $\mathbf{x}_C$ agrees with r. We can repeat this on the domain $V = B$ for the wave equations defining p^B and p^C. This leads to

$$\int_B d\mathbf{x}\left[p^B(\mathbf{x}_B, \mathbf{x})\Delta p^C(\mathbf{x}_C, \mathbf{x}) - p^C(\mathbf{x}_C, \mathbf{x})\Delta p^B(\mathbf{x}_B, \mathbf{x})\right] = w\left[\tfrac{1}{2}p^C(\mathbf{x}_C, \mathbf{x}_B)\right]. \tag{C2}$$

Here, $\mathbf{x}_B = \mathbf{x}_A$ represents s'. Again, we obtain a factor $\frac{1}{2}$ because the delta function is positioned on the boundary of the domain of integration. There is no dependency on p^B in the term on the right-hand side because $\mathbf{x}_C$ lies outside B.

The volume integrals can be treated is the same way as in Appendix B. For eq. (C1), we find

$$w\left[\tfrac{1}{2}p^C(\mathbf{x}_C, \mathbf{x}_A) - p^A(\mathbf{x}_A, \mathbf{x}_C)\right] = \int_{z=z_0} dxdy\left[p^A(\mathbf{x}_A, \mathbf{x})\partial_z p^C(\mathbf{x}_C, \mathbf{x}) - p^C(\mathbf{x}_C, \mathbf{x})\partial_z p^A(\mathbf{x}_A, \mathbf{x})\right]_0^{z_0} = \mathcal{B}\big(p^A(\mathbf{x}_A, \mathbf{x}), p^C(\mathbf{x}_C, \mathbf{x})\big), \tag{C3}$$

whereas eq. (C2) leads to

$$\begin{aligned} w\left[\tfrac{1}{2}p^C(\mathbf{x}_C, \mathbf{x}_B)\right] &= \int_{z=z_0} dxdy\left[p^B(\mathbf{x}_B, \mathbf{x})\partial_z p^C(\mathbf{x}_C, \mathbf{x}) - p^C(\mathbf{x}_C, \mathbf{x})\partial_z p^B(\mathbf{x}_B, \mathbf{x})\right]_{z_0}^{\infty} \\ &= -\mathcal{B}\big(p^B(\mathbf{x}_B, \mathbf{x}), p^C(\mathbf{x}_C, \mathbf{x})\big). \end{aligned} \tag{C4}$$

After adding eqs (C3) and (C4) and using $\mathbf{x}_A = \mathbf{x}_B$, the result is

$$\begin{aligned} w\left[p^C(\mathbf{x}_C, \mathbf{x}_A) - p^A(\mathbf{x}_A, \mathbf{x}_C)\right] &= \mathcal{B}\big(p^A(\mathbf{x}_A, \mathbf{x}), p^C(\mathbf{x}_C, \mathbf{x})\big) - \mathcal{B}\big(p^B(\mathbf{x}_B, \mathbf{x}), p^C(\mathbf{x}_C, \mathbf{x})\big) \\ &= \mathcal{B}\big(p^C(\mathbf{x}_C, \mathbf{x}), p^B(\mathbf{x}_B, \mathbf{x}) - p^A(\mathbf{x}_A, \mathbf{x})\big). \end{aligned} \tag{C5}$$

APPENDIX D: PROOF OF THE REDATUMING RESULT

We show how the combination of source and receiver redatuming provides an expression with $p^B_{r'(s')}$ minus its direct wave $p^{B,\mathrm{dir}}_{r'(s')}$.

We would like to combine eq. (9) with eq. (6). This would lead to an expression containing something like $\mathcal{B}(a, \mathcal{B}(b, c))$, which requires a proper definition of $\partial_z\mathcal{B}(a, c)$. The analogue of eq. (B3) for the z derivatives is

$$w\left[\partial_{z_r} p^C_{r(s)} - \partial_{z_r} p^A_{r(s)}\right] = \int_{z'=z_0} dx'dy'\left[p^A_{s'(s)}\partial_{z'}\partial_{z_r} p^C_{r(s')} - \partial_{z_r} p^C_{r(s')}\partial_{z'} p^A_{s'(s)}\right]. \tag{D1}$$

The integral can be interpreted as an equivalent source term located at $s' = (x', y', z' = z_0)$, based on the wave field p^A for a shot at s, multiplied by the Green's function $\hat{p}^C$ for the domain C, after which the z derivate of the pressure rather than the pressure itself is sampled at the receiver location r. The positions at which the z derivatives are evaluated are made explicit by adding an additional subscript to these derivatives, so $\partial_{z_r} a(\mathbf{x})$ means $\partial_z a(\mathbf{x})|_{z=z_r}$. Eq. (D1) can be abbreviated by

$$w\big[\partial_{z_r} p^C_{r(s)} - \partial_{z_r} p^A_{r(s)}\big] = \mathcal{B}\big(p^A_{s'(s)}, \partial_{z_r} p^C_{r(s')}\big) = \partial_{z_r}\mathcal{B}\big(p^A_{s'(s)}, p^C_{r(s')}\big).$$

Because of the antisymmetry of $\mathcal{B}$, eq. (9) is identical to

$$w\big[p^C_{r(s')} - p^A_{r(s')}\big] = -\mathcal{B}\big(p^B_{r'(s')} - p^{B,\mathrm{dir}}_{r'(s')}, p^C_{r(r')}\big) + \mathcal{B}\big(p^A_{r'(s')} - p^{A,\mathrm{dir}}_{r'(s')}, p^C_{r(r')}\big). \tag{D2}$$

Substitution of this expression into eq. (6) provides

$$w^2\big[p^C_{r(s)} - p^A_{r(s)}\big] = -\mathcal{B}\big(p^A_{s'(s)}, \mathcal{B}\big(p^B_{r'(s')} - p^{B,\mathrm{dir}}_{r'(s')}, p^C_{r(r')}\big)\big) + \mathcal{B}\big(p^A_{s'(s)}, \mathcal{B}\big(p^A_{r'(s')} - p^{A,\mathrm{dir}}_{r'(s')}, p^C_{r(r')}\big)\big). \tag{D3}$$

The second term on the right-hand side of eq. (D3) obeys

$$\mathcal{B}\big(p^A_{s'(s)}, \mathcal{B}\big(p^A_{r'(s')} - p^{A,\mathrm{dir}}_{r'(s')}, p^C_{r(r')}\big)\big) = \mathcal{B}\big(\mathcal{B}\big(p^A_{s'(s)}, p^A_{r'(s')} - p^{A,\mathrm{dir}}_{r'(s')}\big), p^C_{r(r')}\big), \tag{D4}$$

which can be demonstrated by expanding all the terms in the integrals.

Now $\mathcal{B}(p^A_{s'(s)}, p^A_{r'(s')} - p^{A,\mathrm{dir}}_{r'(s')}) = 0$. This can be seen by considering eq. (9) in the special case of a reflection-free domain B. Then $p^C_{r(s')} - p^A_{r(s')} = 0$ and $p^B_{r'(s')} - p^{B,\mathrm{dir}}_{r'(s')} = 0$ because B is reflection free, so $\mathcal{B}(p^C_{r(r')}, [p^A_{r'(s')} - p^{A,\mathrm{dir}}_{r'(s')}]) = 0$. In the last expression, $p^C_{r(s')} - p^A_{r(s')} = 0$ leads to $\mathcal{B}\,(p^A_{r(r')}, [p^A_{r'(s')} - p^{A,\mathrm{dir}}_{r'(s')}]) = 0$. Because this should be independent of the properties of the domain B, we have shown that

$$w^2\big[p^C_{r(s)} - p^A_{r(s)}\big] = \mathcal{B}\big(p^A_{s'(r)}, \mathcal{B}\big(p^C_{r(r')}p^B_{r'(s')} - p^{B,\mathrm{dir}}_{r'(s')}\big)\big), \tag{D5}$$

which finishes the proof.

D1 Remark 1

Although it has been shown that both $p^A_{s'(r)}$ and $\mathcal{B}(p^C_{r(r')}, p^A_{r'(s')} - p^{A,\mathrm{dir}}_{r'(s')})$ lie in the null space of $\mathcal{B}(p^A_{s'(s)}, \cdot)$, which suffices to prove eq. (D5), this does not necessarily mean that the full null space of either $\mathcal{B}(p^A_{s'(s)}, \cdot)$ or $\mathcal{B}(p^A_{s'(r)}, \mathcal{B}(p^C_{r(r')}, \cdot))$ has been characterized. However, for the purpose of redatuming, it is sufficient that any wave related to the domain A has dropped out and does not have to be removed by some filtering operation or up–down decomposition.

D2 Remark 2

We can rewrite eq. (D5) as

$$w^2\big[p^C_{r(s)} - p^A_{r(s)}\big] = \mathcal{B}\big(p^A_{s'(r)}, \mathcal{B}\big(p^A_{r(r')} + \big[p^C_{r(r')} - p^A_{r(r')}\big], p^B_{r'(s')} - p^{B,\mathrm{dir}}_{r'(s')}\big)\big),$$

which may be approximated by

$$w^2\big[p^C_{r(s)} - p^A_{r(s)}\big] \simeq \mathcal{B}\big(p^A_{s'(r)}, \mathcal{B}\big(p^A_{r(r')}, p^B_{r'(s')} - p^{B,\mathrm{dir}}_{r'(s')}\big)\big). \tag{D6}$$

This formula has been used in the examples. The approximation is valid for a short time. Alternatively, one might consider using eq. (D5) for inversion where $p^C_{r(r')}$ is obtained by adding the computed $p^A_{r(r')}$ to the result $p^C_{r(r')} - p^A_{r(r')}$ from the first inversion step. The last result, however, is not complete, as the contribution related to eq. (D4) has dropped out. However, if the redatuming is carried out to a sufficiently large depth, the approximation in eq. (D6) should suffice. Another approach for obtaining $p^C_{r(r')}$ is outlined at the end of Section 2.4.

APPENDIX E: EQUIVALENT SOURCE TERM FOR THE DISCRETE CASE

Here, we rederive the equivalent source term for a second-order finite-difference discretization of the wave equation. This will automatically suggest a discrete representation. The same approach can be generalized to other types of discretizations in a straightforward manner.

A computational grid is defined by the points $x_k = x_{\min} + k\Delta x$ $(k = 0, \ldots, N_x - 1)$, $y_l = y_{\min} + l\Delta y$ $(l = 0, \ldots, N_y - 1)$ and $z_m = z_{\min} + m\Delta z$ $(m = 0, \ldots, N_z - 1)$. The discrete approximation of $p(\omega, x_k, y_l, z_m)$ is denoted by $p_{k,l,m}$. The ω-dependence is not made explicit for brevity. The standard second-order scheme reads

$$-\left(\frac{\omega}{c_{k,l,m}}\right)^2 p_{k,l,m} - D_{xx}p_{k,l,m} - D_{yy}p_{k,l,m} - D_{zz}p_{k,l,m} = f_{k,l,m}, \tag{E1}$$

where

$$D_{xx}p_{k,l,m} = (p_{k+1,l,m} - 2p_{k,l,m} + p_{k-1,l,m})/\Delta x^2,$$
$$D_{yy}p_{k,l,m} = (p_{k,l+1,m} - 2p_{k,l,m} + p_{k,l-1,m})/\Delta y^2,$$
$$D_{zz}p_{k,l,m} = (p_{k,l,m+1} - 2p_{k,l,m} + p_{k,l,m-1})/\Delta z^2.$$

Suppose the domain is cut into two parts at a depth z_0 that lies halfway between z_M and z_{M+1}, so $z_0 = \frac{1}{2}(z_M + z_{M+1})$. To construct the source term, we derive $f_{\mathrm{eq},k,l,m}$ for a discrete solution of the wave equation that is blanked for $z < z_0$. Let $p_{k,l,m}$ be a solution of eq. (E1) for a source term that is zero in the neighbourhood of z_0. The blanked version is

$$q_{k,l,m} = 0, \quad \text{for } m \le M, \qquad q_{k,l,m} = p_{k,l,m}, \quad \text{for } m > M.$$

Without the blanking, substitution of $p_{k,l,m}$ into eq. (E1) leads to a zero source term $f_{k,l,m}$ in the neighbourhood of z_0, assuming that the original point source position $\mathbf{x}_s$ has $z_s < z_0$. With the blanking, we can find the equivalent source term by evaluating eq. (E1) for $q_{k,l,m}$, and using the fact that $p_{k,l,m}$ is a solution of eq. (E1) and that the original source term is zero in the neighbourhood of $z = z_0$. The result is

$$f_{\mathrm{eq},k,l,M} = -p_{k,l,M+1}/\Delta z^2, \quad f_{\mathrm{eq},k,l,M+1} = p_{k,l,M}/\Delta z^2 \tag{E2}$$

and zero elsewhere.

The generalization of this derivation to higher-order finite-difference schemes or finite-element discretizations is straightforward.

The result (E2) can be interpreted as a discrete representation of a delta function and its derivative. A delta function in z that peaks at $z_{\mathbf{M}+\frac{1}{2}}$ can be discretized by

$$\delta\left(z - z_{M+\frac{1}{2}}\right) \simeq \frac{\delta_M + \delta_{M+1}}{2\Delta z},$$

where δ_M is the unit spike at z_M, having the property that the product of δ_M and a grid function of z_m produces its value at $z = z_M$. The derivative of the delta function can be discretized by

$$\delta'\left(z - z_{M+\frac{1}{2}}\right) \simeq \frac{\delta_M - \delta_{M+1}}{\Delta z^2}.$$

With these discrete representations, we find after dropping most of the superscripts and subscripts except the one related to the z coordinate that

$$f_{\mathrm{eq},M+\frac{1}{2}} = \frac{p_M\delta_{M+1} - p_{M+1}\delta_M}{\Delta z^2}$$
$$\simeq -\frac{p_{M+2} - p_{M+1}}{\Delta z}\delta\left(z - z_{M+\frac{1}{2}}\right) - \tfrac{1}{2}(p_{M+1} + p_{M+2})\delta'\left(z - z_{M+\frac{1}{2}}\right) \simeq -\delta(z - z_0)\partial_z p - \delta'(z - z_0)p. \tag{E3}$$

This shows the consistency with eq. (A3).

To go from here to eq. (5), we note that $p = p^A$ was generated by a surface source s and $g = p^C - p^A$ was generated by sources $s'(x, y, z_0)$ at depth $z_0 = z_{M+\frac{1}{2}}$. This implies that

$$g_{r(s)} = p^C_{r(s)} - p^A_{r(s)} \propto \sum_{x',y'} f_{M+\frac{1}{2}} g_{r(s')} \propto \sum_{s'} p^A_{s'(s)} \partial_z g_{r(s')} - g_{r(s')} \partial_z p^A_{s'(s)}.$$

If the wavelet and scaling are properly accounted for, we obtain eq. (6).

APPENDIX F: MINIMUM-NORM SOLUTION

We describe the method for finding the minimum-norm solution of

$$m_1 x_1 + m_2 x_2 = r. \tag{F1}$$

Suppose we want to minimize $|x_1|^2 + \beta^{-2}|x_2|^2$ subject to the constraint (F1). The lagrangian for this problem is

$$\mathcal{L} = \tfrac{1}{2}\left(|x_1|^2 + \beta^{-2}|x_2|^2\right) - \lambda^*(m_1 x_1 + m_2 x_2 - r).$$

Here, λ is the lagrangian multiplier and the asterisk denotes its conjugate. Stationarity of the lagrangian with respect to x_1 and x_2 leads to $x_1 = m_1^* \lambda$ and $x_2 = m_2^* \lambda \beta^2$. Substitution into the constraint provides $\lambda = r/(|m_1|^2 + \beta^2 |m_2|^2)$, so

$$x_1 = \frac{m_1^* r}{|m_1|^2 + \beta^2 |m_2|^2}, \quad x_2 = \frac{\beta^2 m_2^* r}{|m_1|^2 + \beta^2 |m_2|^2}. \tag{F2}$$

The same result can be obtained by considering a least-squares approach to eq. (16):

$$\mathbf{M} \begin{pmatrix} x_1 \\ \gamma^{-1} x_2 \end{pmatrix} = \begin{pmatrix} m_1^* r \\ \gamma^* m_2^* r \end{pmatrix}, \tag{F3}$$

where

$$\mathbf{M} = \begin{pmatrix} m_1 \\ \gamma m_2 \end{pmatrix}^* (m_1 \quad \gamma m_2) = \begin{pmatrix} |m_1|^2 & \gamma m_1^* m_2 \\ \gamma^* m_1 m_2^* & \gamma^2 |m_2|^2 \end{pmatrix}.$$

The singular-value decomposition of $\mathbf{M}$ is

$$\mathbf{M} = Q \begin{pmatrix} |m_1|^2 + |\gamma m_2|^2 & 0 \\ 0 & 0 \end{pmatrix} Q^{-1}, \quad Q = \begin{pmatrix} m_1^* & -\gamma m_2 \\ \gamma^* m_2^* & m_1 \end{pmatrix}.$$

Here, Q has the eigenvectors of $\mathbf{M}$ as columns. The pseudo-inverse of $\mathbf{M}$ is

$$\mathbf{M}^\dagger = Q \begin{pmatrix} (|m_1|^2 + |\gamma m_2|^2)^{-1} & 0 \\ 0 & 0 \end{pmatrix} Q^{-1}.$$

This leads to the following solution of eq. (F3):

$$x_1 = \frac{m_1^* r}{|m_1|^2 + |\gamma m_2|^2}, \quad \gamma^{-1} x_2 = \frac{\gamma^* m_2^* r}{|m_1|^2 + |\gamma m_2|^2}. \tag{F4}$$

For $|\gamma|^2 = \beta^2$, this is the same as the minimum-norm solution of eq. (F2).